Theor Chem Acc (2003) 110: 224–232
Doi 10.1007/s00214-003-0470-2

Theoretical
Chemistry Accounts

Regular article

Theoretical characterization of the absorption spectra of phenanthrene and its radical cation

R. González-Luque[1], **L. Serrano-Andrés**[1], **M. Merchán**[1], **M. P. Fülscher**[2]

[1] Departamento de Química Física, Instituto de Ciencia Molecular, Universitat de València, Dr. Moliner 50, Burjassot, 46100 Valencia, Spain
[2] Department of Theoretical Chemistry, Chemical Center, Lund University, P.O.B. 124, 22100 Lund, Sweden

Received: 11 September 2002 / Accepted: 30 November 2002 / Published online: 6 October 2003

Abstract The vertical absorption spectra of phenanthrene and its radical cation have been studied theoretically by means of a multiconfigurational second-order perturbation approach. Singlet–singlet transition energies and oscillator strengths, and singlet–triplet excitation energies have been studied in the absorption spectrum of phenanthrene up to 6 eV. The absorption spectrum of the phenanthrene radical cation has been computed up to 3.4 eV. The results obtained confirm previous assignments and also lead to new interpretations of the main features of the spectra of these systems.

Keywords: Absorption spectrum – Complete-active-space second-order perturbation theory – Excited states

1 Introduction

Polycyclic aromatic hydrocarbons (PAH) are common products of incomplete combustion processes of petroleum derivatives [1, 2]. Their radical ions were particularly identified as reactive intermediates in soot formation [3]. Because of the high photostability of PAH, they are also considered to be the most abundant free interstellar organic molecules [4]. It has been suggested that a substantial fraction of interstellar carbon may exist in the form of PAH, which may be carriers of the visible, diffuse interstellar absorption band ranging from 4000 Å into the near IR [5, 6]. Detailed knowledge of these processes is important in order to understand the flux of energy in interstellar space and the mechanisms of interstellar chemical reactions. In life sciences PAH have been banned, especially because of their carcinogenic activity [7, 8]. The detection of PAH abundance in biological tissues, flames, atmospheric environments and interstellar space has therefore become a crucial research activity [9], using various spectroscopic methods. The interpretation of the registered data rests on reliable knowledge concerning the excitation energies and oscillator strengths of the isolated molecules.

The optical spectrum of neutral phenanthrene has been studied extensively in the gas phase [10, 11, 12], in solution [13, 14, 15, 16, 17, 18], in the crystalline state [19, 20, 21, 22], and in glass or polymer matrices [23, 24, 25, 26, 27]. The experimental techniques include one-photon [10, 11, 23, 24, 25, 28] and two-photon [16, 26] absorption spectroscopy, magnetic circular dichroism (MCD) [29], and electron energy loss spectroscopy (EELS) [19]. In addition, the triplet-triplet absorption spectra [30, 31, 32, 33, 34, 35, 36] and the electron spin resonance spectrum [37] of the lowest triplet states have been reported. The spectroscopic data available on phenanthrene radical cations have been obtained from photoelectron spectroscopy and phenanthrene suspended in matrices [25, 27, 38, 39, 40, 41].

The UV/vis optical absorption spectrum of neutral phenanthrene in the gas phase and in solution was expected to have a structure similar to that of other acenes. It is therefore common practice to label the low-lying excited states according to Platt's scheme [42]. In phenanthrene, the first band (3.5–3.8 eV), denoted ^1L_b, is extremely weak ($\epsilon = 200$ cm^{-1} M^{-1} in cyclohexane), short-axis polarized (z direction in Fig. 1), and has a well-resolved vibrational structure. The next band in energy (^1L_a) is also weak ($\epsilon = 14000$ cm^{-1} M^{-1}), but long-axis polarized, and placed around 4.3 eV. A strong band ($\epsilon = 60000$ cm^{-1} M^{-1}) with a maximum at about 5.0 eV is commonly believed as being related to two transitions: the ^1B_a and ^1B_b bands, short-axis and long-axis polarized respectively. The B bands are so close to each other that the weaker ^1B_b band seems to be hidden in ordinary absorption spectra. However, two transitions are clearly observed in stretched-polymer sheets [23], in the MCD spectrum [29], and in the two-photon

Contribution to the Björn Roos Honorary Issue

Correspondence to: L. Serrano-Andrés
e-mail: luis.serrano@uv.es
Permanent address: M. P. Fülscher,
Department of Clinical Chemistry,
Malmö University Hospital, 20502 Malmö, Sweden

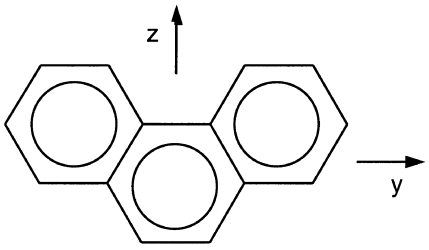

Fig. 1. Structure of the phenanthrene molecule

excitation spectrum of phenanthrene in ethanol [16]. The strongest two-photon band is assigned to the ^1B_b ($^1B_2$ symmetry) state, not seen directly in the UV spectrum. The next highest region of the absorption spectrum, around 5.7 eV, contains two medium intensity bands ($\epsilon = 23000$ and 35000 cm^{-1} M^{-1} in ethanol), which have transitions related to states of different symmetry. Eight transitions to singlet states have been identified below around 6 eV [11, 16, 19, 23, 29]. There are a number of unassigned transitions, some of them hidden in the optical spectrum. The situation is even more complex for the singlet-triplet transitions, where the nature and symmetry of the low-lying triplet state are still not properly determined.

The two lowest bands in the photoelectron spectrum of phenanthrene [39, 40, 41] are reported at 7.86 and 8.15 eV. Thus, the lowest-energy transition from the 1^2B_1 ground state of the radical cation, lies in the IR range, 0.29 eV, and it has not been measured in the optical spectrum of phenanthrene radical cation embedded in matrices [25, 27, 38]. At energies below 2 eV, the optical spectrum of the phenanthrene radical cation is dominated by a strong absorption system assigned to the $1^2B_1 \rightarrow 2^2A_2$ transition, having a rich vibrational structure. Furthermore, a weak absorption band is observed at about 2 eV. At energies above 2 eV four absorption band systems can be identified, with the most intense transition located at about 2.9 eV in the matrix spectrum. The observed vibrational energy levels of all the band systems are basically independent of the experimental technique and the environment, which is not expected to largely perturb the geometry of the states upon excitation.

Assignments and characterizations of the electronic transitions in phenanthrene are almost exclusively based on calculations employing Hückel, Pariser–Parr–Pople (PPP)-SCF, AM1 or CNDO/S molecular orbital (MO) theories [13, 19, 27, 29, 31, 43, 44, 45, 46, 47, 48, 49]. Although these studies led to qualitative interpretations of the absorption spectra, they do not provide a conclusive rationalization of the electronic spectrum of phenanthrene. A quantitative prediction of the electronic spectra of conjugated systems requires ab initio methods taking into account electron correlation. To the authors' best knowledge there exists only one paper reporting applications of ab initio methods to study the electronic absorption spectrum of phenanthrene radical cation [50], but there the results had to be corrected by a redshift of 0.4 eV to obtain a proper interpretation of the spectrum.

The present study has been undertaken in order to provide an improved theoretical description of the electronic spectra of phenanthrene and its radical cation. In this paper, we present an ab initio study of the electronic transitions of phenanthrene and the phenanthrene radical cation in order to give quantitative reliable vertical excitation energies for the main valence states. In phenanthrene, up to 12 singlet and 12 triplet vertically excited valence states have been characterized. Eight doublet states of the radical cation (up to an energy of 3 eV) have been computed. The spectroscopic study was performed within the framework of multiconfigurational second order perturbation theory [51, 52], the so-called CASSCF/CASPT2 approach. The suitability of the CASSCF/CASPT2 method in computing differential correlation effects, especially for excitation energies, has been illustrated in a number of earlier applications [53, 54, 55].

2 Methods

The geometries of phenanthrene and its radical cation were optimized at the B3LYP/6-31G* level of theory. All calculations were carried out within C_{2v} symmetry. The molecule was placed in the yz plane with the twofold symmetry axis of the molecule along the z-axis. To characterize the excited states we used a multiconfigurational second-order perturbation theory, the CASPT2 method [51, 52]. The CASSCF procedure determines the multiconfigurational reference function employed in the perturbational treatment. The CASSCF/CASPT2 calculations used generally contracted basis sets of atomic natural orbital type. They were obtained from C(10s6p3d)/H(7s) primitive sets [56] by employing the contraction scheme C[3s2p1d]/H[2s]. To calculate the excitation energy of the lowest Rydberg state in the phenanthrene neutral molecule, the basis set was supplemented with two s-type and two p-type diffuse function (see exponents in Refs. [57, 58]) placed at the charge centroid of the molecule. The MOs of the excited states were obtained from state-average CASSCF calculations, where the averaging includes all states of interest of a given symmetry. The natural choice for the active space in phenanthrene is 14 valence π orbitals with 14 active electrons. To compute the Rydberg state, the active space must be extended to include the 3s Rydberg orbital. Full configuration interaction expansions of 14 electrons in 15 active orbitals are at the limit of the current implementation of the CASSCF method. Therefore, a reduction of the active space for the study of the electronic spectrum was performed. The π space was reduced to 12 orbitals by taking out one virtual orbital of each symmetry. The active space is denoted (14/0606), where the first entry gives the number of active electrons and the following entries indicate the number of active orbitals in each of the four irreducible representations (a_1, b_1, b_2, a_2) of the C_{2v} symmetry point group. An active space (14/1606) was employed to compute the 1^1B_1(3s) Rydberg state. In the phenanthrene radical cation calculations an active space (13/0707) was employed. All calculations were referred to the corresponding ground state computed with the equivalent active space. A level shift corrected perturbation theory [53, 54] was introduced to handle intruder states weakly interacting with the CASSCF reference function. An extensive test of this approach for spectroscopic applications is available in the literature [59]. A level shift of 0.3 au was applied in the neutral system. The dipole transition moment was computed by using the CASSCF state interaction method, which enables the efficient calculation of the transition properties for nonorthogonal state functions [60, 61]. Energy differences corrected by CASPT2 correlation energies were used in the oscillator strength formula. Calculations were performed using Gaussian94 [64] and MOLCAS-4 quantum chemistry software [63].

3 Results and discussion

3.1 The singlet–singlet spectrum of neutral phenanthrene

In order to get a better understanding of the most important features of the electronic spectrum of phenanthrene, an analysis of the MO distribution can be helpful. The orbital energy levels close to the highest occupied π MO, HOMO (H), and lowest unoccupied π^* MO, LUMO (L), calculated at the SCF level (canonical MOs) are depicted in Fig. 2. The low-lying electronic spectrum of neutral phenanthrene is determined to a large extent by the five highest occupied orbitals and the four lowest unoccupied orbitals. These are separated by more than 1.8 eV from the rest. The calculations place the two highest occupied MOs (H, H-1), of b_1 and a_2 symmetry, respectively, close in energy (0.32 eV). The two lowest unoccupied orbitals (L,L + 1) of a_2 and b_1 symmetry, respectively, are nearly degenerate, with a splitting of 0.03 eV. These four orbitals are involved in the main configurations of the excited states of phenanthrene. The remaining valence antibonding π^* orbitals have a pronounced energy separation with respect to these orbitals, more than 1 eV. Because of the structure of the MOs, a number of electronic transition energies are expected to be found in a narrow region. In spite of its qualitative character, the MO distribution obtained at the SCF level represents a useful tool for the interpretation of the findings obtained by using more advanced (and complex) wave functions.

The main contributions to the CASSCF wave functions calculated for the valence singlet states of phenanthrene are compiled in Table 1. The configurations with coefficients larger than 0.05 have been classified in three groups, according to the number of replacements (single, double, triple) with respect to the main configuration of the ground state. The number of configurations and the weights for each group are reported on the right-hand side of the table. Only configurations with a weight larger than 10% are listed. In order to simplify the notation, they are described as electronic excitations from the main configuration of the ground state.

The results obtained by means of the CASSCF/CASPT2 procedure are collected in Table 2. The first column identifies the excited states of phenanthrene. The second and third columns report the vertical excitation energies computed at the CASSCF and CASPT2 levels, respectively. The differences between the two energies are a measure of the contribution of the differential dynamic correlation contributions to the energy of the states. The available experimental data are listed in the fourth column. Finally, the calculated oscillator strengths as well as the experimental values for the extinction coefficient are compiled.

The lowest-lying singlet excited state of phenanthrene has $^1A_1$ symmetry. The CASSCF wave function is dominated by the $3a_2 \rightarrow 4a_2$ and $4b_1 \rightarrow 5b_1$ one-electron configurations (see Table 1). In terms of the one-electron levels (see Fig. 1) they correspond to the promotions H-1 → L and H → L + 1. The computed CASPT2 vertical excitation energy is 3.42 eV. The maximum of this very weak band has been found near 3.7 eV in the gas phase [10, 11, 12], at 3.63 eV in neon and argon matrices [25, 26], and at 3.5–3.6 eV in solution [14, 15, 16]. This transition corresponds to the lowest-energy band in the UV spectrum, and it is a short-axis polarized band with low intensity, but with a well resolved 0-0 transition. The band shows rich vibrational structure and most of the vibrations involved are totally symmetric [16]. It is assigned to the symmetry-allowed, pairing-forbidden transition $1^1A_1^- \rightarrow 2^1A_1^-$, labeled ^1L_b. In phenanthrene, as in other acenes and related compounds [57, 64, 65], the integrated oscillator strength of this band obtained from the solution spectrum is quite small, approximately 0.003 [13, 29]. Other calculations performed with semiempirical methods confirm the assignment. While the PPP method [44] reports an excitation energy of 3.35 eV, similar to that obtained by CASPT2, the CNDO/S studies [16, 19, 66] tended to overestimate the excitation values.

The next two lowest-lying singlet excited states, 1^1B_2 and 2^1B_2, are involved in the description of the second-energy band observed experimentally between 4.1 and 4.5 eV. These states have singly excited character, with a total weight of single excited configurations larger than 75%. The nature of the 1^1B_2 state, with clear multiconfigurational character, is complex. Five configurations participate in the composition of the wave function by more than 10%. On the other hand, in the description of the CASSCF 2^1B_2 state wave function, there is one predominant configuration, $4b_1 \rightarrow 4a_2$ (39%), corresponding to the H → L promotion. When comparing this wave function with those of other acenes [42, 57, 64, 65], the 2^1B_2 transition can be clearly related to Platt's ^1L_a band. The presence of two states of the same symmetry at very similar energies, computed 4.26 and 4.37 eV, is a consequence of the near degeneracy of the LUMO and LUMO + 1 MOs. In this region, only one transition can be identified in the one-photon absorption spectrum of phenanthrene [10, 11, 16, 19, 29] and was assigned as an excitation from the ground state to a $^1B_2$ state, with a band origin reported at 4.24 eV in ethanol [16], hexane [15], and in two-photon [16] and EELS [19] spectra, and a maximum placed at 4.31 eV in argon matrices [26] and at 4.36 eV in the gas phase [10] and neon matrices [25]. The CASPT2 energies for the 1^1B_2 and 2^1B_2 transitions are 4.26 and 4.37 eV, with oscillator strengths 0.000 and 0.038, respectively. Clearly, the optically intense transition corresponds to the 2^1B_2 state, computed at 4.37 eV. Considering the composition of the CASSCF wave function, this is Platt's ^1L_a band. The location of the other $^1B_2$ state seems more problematic. Several semiempirical PPP calculations [28, 43] already predicted the presence of a second transition to a $^1B_2$ state, first observed in 1,10-phenanthroline [28]. In the MCD [29] and two-photon spectra [16] a second $^1B_2$ transition was reported in the energy range 4.4–4.6 eV. On the other hand, Salama et al. [25] detected a band origin at 4.53 eV in the neon matrix spectrum and this was attributed to a new $^1B_2$ transition. The CASPT2 result places the transition to the 1^1B_2 state below (vertically) the 2^1B_2 (^1L_a) intense transition only

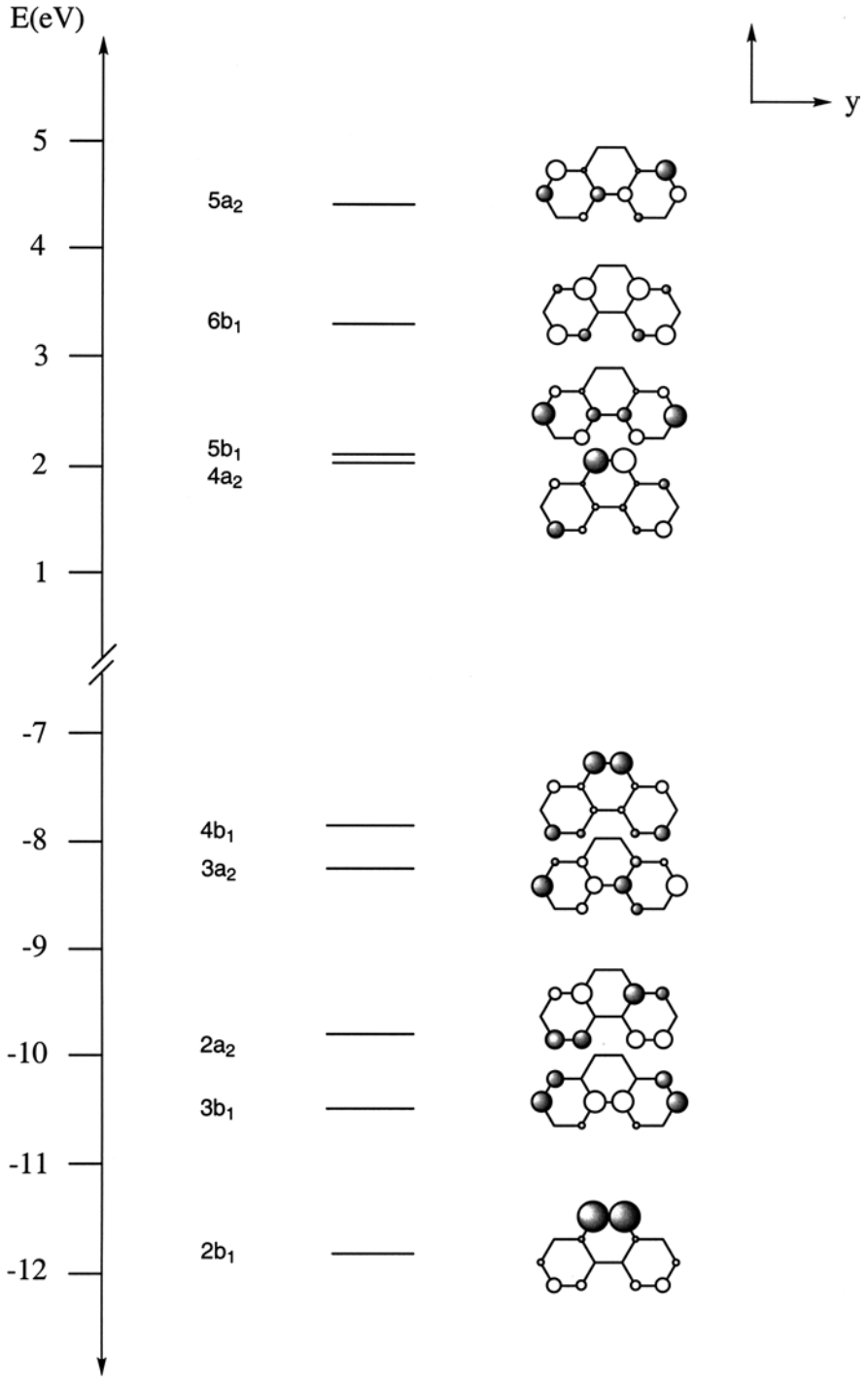

Fig. 2. Most relevant π canonical Molecular orbitals self-consistent-field orbital energies computed with the atomic natural orbital type C [3s2pld]/H [2s] basis set for the phenanthrene molecule

by 0.11 eV. It is no doubt that both transitions overlap in the same group of bands, but their relative position is difficult to establish. The transition to the 1^1B_2 state is very weak, both in the one-photon and in the two-photon spectra [16]. It is possible that it remains undetected and that the features observed near 4.4–4.5 eV are simply progressions of the more intense 2^1B_2 transition.

The 3^1A_1, 3^1B_2, and 4^1A_1 excited states, are involved in the description of the third band of the observed one-photon spectrum [10, 11, 15, 25, 29] between 4.7 and 5.2 eV. It is clear that the transition from the ground state to the 3^1B_2 state, computed at the CASPT2 level at 4.81 eV with oscillator strength 1.218, corresponds to the most intense feature of the spectrum. The wave function of this state is dominated by the H-1→L+1 excitation, which clearly leads to assigns the related transition as Platt's ^1B_a band. This transition was erroneously coined as ^1B_b [13]. The band maximum has been reported at 4.88 eV in solution [14], at 4.95 eV in hexane and ethanol [15, 16], at 5.00 eV in argon matrices [26], at 5.10 eV in neon matrices [25], and at 5.19 eV in the gas phase [11]. In the low-energy tail of the band another transition is assigned to the 3^1A_1 state

Table 1. Complete-active-space self-consistent-field (*CASSCF*) wave function for the computed singlet states of neutral phenanthrene. Configurations contributing with a coefficient larger than 0.05 have been considered

State	Configuration[b,c]	w/%	No. conf. (weight)[a]		
			S	D	T
$2^1A_1(^1Lb)$	$(3a_2)\rightarrow(4a_2)$	33	2(1%)	16(9%)	
	$(4b_1)\rightarrow(5b_1)$	36			
1^1B_2	$(3a_2)\rightarrow(5b_1)$	14	7(75%)	15(6%)	
	$(2a_2)\rightarrow(5b_1)$	20			
	$(3a_2)\rightarrow(6b_1)$	10			
	$(4b_1)\rightarrow(4a_2)$	15			
	$(3b_1)\rightarrow(4a_2)$	10			
$2^1B_2(^1L_a)$	$(3a_2)\rightarrow(5b_1)$	14	8(78%)	9(4%)	
	$(3a_2)\rightarrow(6b_1)$	11			
	$(4b_1)\rightarrow(4a_2)$	39			
3^1A_1	$(2a_2)\rightarrow(4a_2)$	34	21(54%)	11(25%)	
	$(4b_1)\rightarrow(6b_1)$	12			
	$(4b_1)^2\rightarrow(6b_1)^2$	13			
$3^1B_2(^1B_a)$	$(3a_2)\rightarrow(5b_1)$	52	6(78%)	8(5%)	5(2%)
	$(4b_1)\rightarrow(4a_2)$	23			
$4^1A_1(^1B_b)$	$(3a_2)\rightarrow(4a_2)$	35	7(75%)	17(8%)	2(1%)
	$(4b_1)\rightarrow(5b_1)$	35			
4^1B_2	$(4b_1)\rightarrow(5a_2)$	10	11(49%)	19(28%)	
	$(2b_1)\rightarrow(4a_2)$	10			
	$(3b_1)\rightarrow(4a_2)$	13			
5^1A_1	$(3a_2)\rightarrow(5a_2)$	14	8(48%)	21(31%)	
	$(3b_1)\rightarrow(5b_1)$	30			
	$(3a_2)^2\rightarrow(5b_1)^2$	20			
6^1A_1	$(2b_1)\rightarrow(5b_1)$	21	11(36%)	26(31%)	1(1%)
5^1B_2	$(2b_1)\rightarrow(4a_2)$	19	9(51%)	20(28%)	
	$(3b_1)\rightarrow(4a_2)$	15			
6^1B_2	$(2a_2)\rightarrow(5b_1)$	22	9(57%)	19(22%)	1(1%)

[a] Number, type [single (S), double (D), triple (T)] and weight (%) of the excitations
[b] Main configurations displayed (>10%)
[c] $3a_2$ (HOMO-1), $4b_1$ (HOMO), $4a_2$ (LUMO), $5b_1$ (LUMO + 1)

Table 2. Computed vertical excitation energies (eV), oscillator strengths *f*, and experimental data for the singlet–singlet transitions of neutral phenanthrene

State	Excitation energies			f[a]
	CASSCF	CASPT2	Experimental	
$2^1A_1(^1L_b)$	4.25	3.42	3.51[b], 3.58[c,d], 3.63[e,f], 3.68[g]	0.000 (250)[c]
1^1B_2	5.68	4.26	4.4–4.6[h,i], 4.53[e], 4.59[f]	0.000
$2^1B_2(^1L_a)$	6.14	4.37	4.09[b], 4.24[c,d,h,j], 4, 31[f], 4.36[e,g]	0.038(14800)[c]
3^1A_1	6.36	4.56	4.84[f], 4.64[i], 4.70[h], 4.73[e]	0.268
$3^1B_2(^1B_a)$	6.94	4.81	4.88[b], 4.95[c,d], 5.00[f], 5.10[e], 5.19[g]	1.218(67000)[c]
$4^1A_1(^1B_b)$	6.57	5.00	5.02[h]	0.011
$1^1B_1(3s)$	5.23	5.42		0.002
4^1B_2	7.22	5.49	5.41[e]	0.003
5^1A_1	6.81	5.75	5.60[h]	0.000
6^1A_1	7.14	5.75	5.63[c], 5.68[j], 5.74[f]	0.012(23000)[c]
5^1B_2	7.56	5.78		0.005
6^1B_2	8.18	5.92	5.78[e], 5.86[b,c,j], 5.98[f]	0.333(35000)[c]

[a] Computed values. Experimental molar extinction coefficients ($cm^{-1}M^{-1}$) in parentheses
[b] Solution absorption spectrum [14]
[c] Absorption spectrum in ethanol. 0–0 transition [16]
[d] Absorption spectrum in hexane [15] and cyclohexane [18]
[e] Absorption spectrum in neon matrices [25]
[f] Absorption spectrum in argon matrices [26]
[g] Gas-phase absorption spectrum [10, 11, 12]
[h] Two-photon absorption spectrum [16]
[i] Magnetic circular dichroism spectrum [29]
[j] Electron- energy- loss spectrum [19]

at 4.56 eV with oscillator strength 0.268. This band was not reported in the optical spectrum, but it has been described in stretched-polymer [23, 28] and in the MCD [29] phenanthrene spectra at 4.75 and 4.64 eV, respectively. Dick and Hohlneicher [16] observed a strong two-photon absorption to a $^1A_1$ state at 4.70 eV. In view of these results, Salama et al. [25] attributed to this transition the progressions detected at 4.73 eV. The largest contributions to the CASSCF wave function derive from the H-2→L and H→L + 2 excitations, and include the important participation of doubly excited configurations. It indicates that the 3^1A_1 state does not match with the ^1B_b state in Platt's scheme. In contrast, the 4^1A_1 state has a CASSCF wave function with a clear

mixture (35% each) of the H-1→L and H→L+1 configurations, in agreement with the character of the ^1B_b state. Here too, the near degeneracy of the L and L+1 orbitals is responsible for the presence of two states of similar excitation energy. The 4^1A_1 transition is predicted to peak at 5.00 eV with oscillator strength 0.011. Two-photon spectroscopy [16] is the only experimental technique which has been able to detect a transition on the high-energy side of the intense 3^1B_2 band. The clear feature observed at 5.02 eV can be assigned to the CASPT2 4^1A_1 transition.

Comparing the low-lying spectrum of phenanthrene with spectra from other acenes, such as naphthalene [57] or anthracene [67], several differences can be noted. The set of Platt's bands ^1L_b, ^1L_a, ^1B_a, and ^1B_b, appear at 4.03 (0.00), 4.56 (0.05), 5.54 (1.34), and 5.93 eV (0.31), respectively, in naphthalene [57] (oscillator strengths within parentheses). In phenanthrene, where the system is enlarged, there is a general decrease of the excitation energies, although the ratio among the intensities is quite similar, except for the ^1B_b band in phenanthrene, where the relative intensity decreases. The structure of the spectrum in anthracene is different. The bands are computed [67] at a multiconfigurational perturbation level at 3.23 (0.00), 3.40 (0.08), 5.67 (0.14), and 4.77 eV (1.94), respectively. The main differences observed with respect to phenanthrene is the change in the energy and intensity order in the ^1B_a and ^1B_b bands. The states are much more separated in anthracene and there is no near degeneracy in the orbital energies of the H, H+1 or L, L+2 orbitals.

Most of the spectra of phenanthrene were registered in condensed phases, where Rydberg transitions are not present or highly perturbed. The low-lying Rydberg transition (HOMO→3*s*) is here predicted at 5.42 eV, with a computed oscillator strength of 0.002. Close to it, the transition to the 4^1B_2 state is obtained at 5.49 eV with a similar oscillator strength. This band will most probably be hidden on the high-energy side of the 3^1B_2 band or the low-energy tail of higher bands. A band has been reported with an origin at 5.41 eV in the neon matrix spectrum [25]. Most probably it can be assigned to the valence 4^1B_2 transition instead of to a Rydberg feature, which is expected to be perturbed in the matrix.

The next band in energy in the optical spectrum of neutral phenanthrene has two clear components identified in the EELS spectrum at 5.68 and 5.86 eV [19]. Similar peaks were described in the optical spectrum in ethanol, 5.63 and 5.86 eV [16], in increasing order of intensity. Only one transition at 5.78 eV is, however, reported in the neon matrix spectrum [25]. Four excited singlet states can be related to this set of bands: 5^1A_1, 6^1A_1, 5^1B_2 , and 6^1B_2, with excitation energies computed at 5.75, 5.75, 5.78, and 5.92 eV, respectively. The $1^1A_1 \rightarrow 6^1A_1$ and $1^1A_1 \rightarrow 6^1B_2$ excitations carry most of the intensity, mainly the latter, computed with an oscillator strength of 0.333. These two transitions can be clearly assigned to the bands observed in the one-photon spectra (see Table 2). Dick and Hohlneicher [16] also identified an intense $^1A_1$ transition in the two-photon spectrum at 5.60 eV. In order to fulfill the mutually exclusive pairing selection rules, we assign this two-photon intense transition to the 5^1A_1 state computed at 5.75 eV, and it is practically forbidden in the one-photon spectrum. The corresponding CASSCF wave function of the 5^1A_1 state has large contributions of doubly excited configurations.

Previous semiempirical calculations on the absorption spectrum of neutral phenanthrene gave contradictory pictures. PPP calculations [44] produced results similar to those obtained at the CASPT2 level (with clear disagreements in the assignments). In contrast, CNDO/S results [1] overestimate the excitation energies, and they show a marked dependency on the different selected configuration interaction expansions.

3.2 The singlet–triplet spectrum of neutral phenanthrene

The location and nature of the lowest-lying triplet state in phenanthrene are well known. The transition in the phosphorescence spectrum of phenanthrene appears at 2.69 eV diethyl ester–isopentane–ethanol (EPA) in (0-0), at 2.65 eV in biphenyl [10, 20], and at 2.70 eV in the EELS spectrum [19]. The CASPT2 excitation energy of the 1^3B_2 (T_1) state is 2.66 eV, in agreement with experimental evidence. There have been several attempts to locate higher triplet states. No conclusive assignments have been obtained, however [19]. In particular, the position and nature of the second triplet state are still in debate [19, 68]. The second and third triplet states have been observed by EELS spectroscopy at 3.04 and 3.45 eV [19]. In accordance with our computed results we assign the two EELS peaks to the 2^3B_2 and 1^3A_1 states, computed at 3.24 and 3.30 eV.

The assignment of higher triplet states [19] is based on a comparison of calculated triplet energies and intensities from the triplet–triplet absorption spectrum [30, 31, 69, 70]. Only the symmetry of the triplet state at 5.23 eV is well characterized. The triplet–triplet transition found from T_1 at 2.55 eV is strong enough to measure its polarization [69] and to determine the $^3A_1$ symmetry of the final state. Other measurements of the triplet–triplet spectra of phenanthrene in rigid glasses [30, 31] reported excited triplet states at 4.19, 4.38, 4.58, and 4.76 eV. The effect of solvent on the more intense transitions of the triplet–triplet electronic transitions of phenanthrene was analyzed by Del Barrio et al. [70]. A shift of 0.17 eV to the red is obtained in a polar solvent such as ethanol with respect to the gas-phase datum. Our assignment of higher triplet states (Table 3) is based on the calculated triplet energies from triplet–triplet absorption spectra [30, 31, 70]. The assignment of the 5^3A_1 state as being responsible of an intense transition in the triplet–triplet spectrum seems clear. The computed energy value at 5.46 eV agrees with the transition located in the gas phase at 5.40 eV [31], and in ethanol at 5.23 eV [70]. Moreover, the symmetry of the state, $^3A_1$, correlates with that determinated from the polarization measurements [69]. The 6^3A_1 state has a computed energy of 5.55 eV, in agreement with the experimental data (Table 3).

3.3 The absorption spectrum of phenanthrene radical cation

The lowest bands in the photoelectron spectrum of phenanthrene [39] have been reported at 7.86, 8.15, 9.28, 9.89, and 10.59 eV. At the neutral molecule geometry, the ground state of the radical cation has $^2B_1$ symmetry. The low-lying transition of the cation lies then in the IR range, at 0.29 eV from the 1^2B_1 ground state. Three more transitions, placed at 1.42, 2.03, and 2.73 eV, can therefore be deduced from the photoelectron spectrum [39]. The low-lying transition in the IR spectrum was not reported in the optical absorption spectrum of phenanthrene in a neon matrix [25] or in a boric acid glass [27]. Six band systems were recorded in the range 1.38–3.59 eV. Those at 1.4 and 2.9 eV are the most intense ones. There are large discrepancies between theoretical and experimental oscillator strengths for the phenanthrene radical cation. Both semiempirical and ab initio values [41, 50] are 3 or 4 orders of magnitude higher than those measured in matrices by Salama et al. [25], who suggested a revision of the theoretical results. Recently, Bréchignac and Pino [71] designed a new model to estimate cross-sections, and therefore oscillator strength values, from direct measurements in the matrix. The $1^2B_1 \rightarrow 2^2A_2$ transition in the absorption spectrum of the phenanthrene radical cation in an argon matrix was measured with an oscillator strength of 0.15 ± 0.05 [71]. This value, although approximate, is considered to be more realistic than the small value estimated by Salama et al. [25] and it is closely related to the values obtained by the theoretical methods. Our results also support the most recent estimations. The finding that the oscillator strengths of the electronic transitions in PAH cations can have relatively large values is important in the discussion of the role of PAH as carriers of the diffuse absorption in interstellar media [71]. Otherwise, an unrealistic abundance of PAH will be required.

Table 3. Computed vertical singlet–triplet excitation energies (eV) and experimental data of neutral phenanthrene

State	Excitation energies		
	CASSCF	CASPT2	Experimental
1^3B_2	3.53	2.66	2.70[a], 2.65[b]
2^3B_2	4.33	3.24	3.04[a]
1^3A_1	4.39	3.30	3.45[a]
2^3A_1	4.87	3.80	
3^3A_1	5.83	4.02	
3^3B_2	5.33	4.07	4.19[c]
4^3A_1	5.43	4.32	4.38[c]
4^3B_2	5.87	4.66	4.58[c]
5^3B_2	6.97	4.92	4.76[c]
6^3B_2	6.78	4.93	
5^3A_1	7.32	5.46	5.40[d], 5.23[e]
6^3A_1	7.03	5.55	5.57[d], 5.41[e]

[a] Electron energy loss spectrum [19]
[b] Phosphorescence spectrum [10, 20]
[c] From triplet–triplet absorption in rigid glasses [30, 31]
[d] From triplet–triplet absorption in the vapor [70]
[e] From triplet–triplet absorption in ethanol [70]

To assign the experimentally observed band maxima we report calculations of the excited states of the phenanthrene radical cation both at the geometry of the neutral molecule and at the optimized geometry of the cation. It is assumed that the data obtained from the photoelectron spectra better correspond to the transition energies computed at the neutral geometry (hereafter NEU), while the values reported in the neon matrix spectrum match the transitions computed at the radical cation ground-state geometry (hereafter CAT). The results are compiled in Table 4.

The transition from the 1^2B_1 to the 1^2A_2 state was computed at the CASPT2 level at 0.27 and 0.57 eV at the NEU and CAT geometries, respectively, both with very small oscillator strengths. This transition, which lies in the IR range, corresponds to the lowest energy difference found between the two lowest bands of the photoelectron spectrum of phenanthrene [39], 0.29 eV, and matches the computed lowest-lying transition to the 1^2A_2 state at 0.27 eV using the neutral phenanthrene geometry (NEU). The second computed transition to the 2^2A_2 state at 1.22 (NEU) and 1.39 eV (CAT) has larger oscillator strengths at both geometries: 0.079 (NEU) and 0.068 (CAT). The photoelectron [39] and the neon and boric acid glass matrix spectra [25, 27] report a transition at 1.42 and 1.38 eV, respectively.

We found a number of excited states with energies higher than 2 eV. We assigned the two features of the photoelectron spectra [39] at 2.03 and 2.73 eV to the 2^2B_1 and 3^2B_1 states, respectively. Focusing on the data obtained in a neon matrix a transition is reported at 1.95 eV [25], corresponding to the excitation to the 2^2B_1 state with a small oscillator strength, 0.002. This is probably the reason why it is not observed in the boric acid glass spectrum [27]. The remaining computed transitions are observed both in the neon matrix [25] and in the boric acid glass [27] spectrum, with similar values. The most intense band is predicted to correspond to the 3^2A_2 state at 2.86 eV, computed at the cation geometry. At the neutral molecule geometry the most intense transition corresponds to the 4^2A_2 state, at 3.13 eV. The results computed by Niederalt et al. [50] at the MRDCI level, including a general correction (redshift) of 0.4 eV, agree in general with our results both in energy and intensity. These authors computed, however, the transitions to both 4^2A_2 and 4^2B_1 as being degenerate at 3.96 eV. This is not found in the experimental spectra and can be ruled out in view of the present results, where the two states are predicted to be spaced by about 0.2 eV (Table 4).

4 Summary

We have presented an ab initio study of the electronic spectra of phenanthrene and its radical cation. The study was performed using multiconfigurational second-order perturbation theory, the so-called CASSCF/CASPT2 method. To our knowledge, this is the first ab initio study of the neutral phenanthrene spectrum. This is a molecule that has received a lot of attention from the experimental side. Optical absorption, one-photon and two-photon spectroscopies in different media, MCD, and EELS

Table 4. Computed vertical excitation energies (eV), oscillator strengths *f*, and experimental data for the doublet–doublet transitions of the phenanthrene radical cation. Geometries of both neutral phenanthrene and the radical cation were used

State	Neutral geometry			Cation geometry			Experimental	
	Excitation energies		*f*	Excitation energies		*f*		
	CASSCF	CASPT2		CASSCF	CASPT2		Photo[a]	Absorption
1^2B_1								
1^2A_2	0.12	0.27	0.0001	0.55	0.57	0.0004	0.29	
2^2A_2	1.42	1.22	0.079	1.64	1.39	0.068	1.42	1.38[b,c]
2^2B_1	2.02	1.82	0.001	2.36	2.03	0.002	2.03	1.95[c]
3^2B_1	2.80	2.49	0.036	2.94	2.56	0.028	2.73	2.55[b],2.63[c]
3^2A_2	3.65	3.12	0.011	3.59	2.86	0.187		2.87[b],2.91[c]
4^2B_1	4.15	3.37	0.049	4.17	3.14	0.056		3.07[b],3.13[c]
4^2A_2	3.91	3.13	0.129	3.95	3.32	0.049		3.53[b],3.59[c]

[a] Photoelectron spectrum [39]
[b] Absorption spectrum in boric acid glasses matrices [27]
[c] Absorption spectrum in neon matrices [25]

spectroscopies have been used to find the basic structure of the spectrum. The assignment of the bands is difficult. Several of the $^1B_2$ transitions are too weak to be observed in the optical spectrum, while they are observed in the MCD spectrum or in stretched-polymer spectra (see references in previous sections). A similar situation occurs for some of the $^1A_1$ peaks, which are only observed in the two-photon spectra. The computed results help in the interpretation of the main features of the spectrum and confirm or rule out certain tentative assignments proposed in the literature. In particular, assignment of the four Platt bands, ^1L_b, ^1L_a, ^1B_a, and ^1B_b, to the 2^1A_1, 2^1B_2, 3^1B_2, and 4^1A_1 transitions has been proposed. The singlet–triplet spectrum has also been computed and a number of new assignments have been performed. Finally, we have calculated the vertical absorption spectra of the phenanthrene radical cation. Two geometries were used in the calculations: the optimized ground-state geometries of the neutral molecule and of the radical cation. In this way it is possible to compare the experimental data obtained from photoelectron spectroscopy and from optical absorption. The former are assumed to better match the spectrum computed at the neutral molecule geometry, while the optical absorption data can be better related to the spectrum computed at the cation geometry. Our calculations confirm that previous experimental estimations of the oscillator strength values for the phenanthrene radical cation of about 10^{-5} [25] were not correct, and support more recent studies [71] where the values rise to more than 10^{-1} for some of the transitions. The current results confirm that PAH, and in particular their cations, can be efficient carriers for the diffuse absorption band observed from the visible to the near-IR range in the interstellar medium.

Acknowledgements. The research reported in this paper was supported by project BQU2001-2926 of the Spanish MCYT, the Generalitat Valenciana, and the Swedish Foundation for Strategic Research (SSF). The paper is dedicated to our friend and colleague, Prof. Björn O. Roos in appreciation of his outstanding contributions to quantum chemistry in general and excited-state quantum chemistry in particular.

References

1. Ramdahl T, Bjorseth J (1985) Handbook of polycyclic Aromatic Hydrocarbons. Marcel Dekker, New York
2. Kislov VV, Mebel AM, Lin SH (2002) J Phys Chem A 106: 6171
3. Frenklach M, Warnatz J (1987) Combust Sci Technol 51: 265
4. Salama F, Allamandola LJ (1992) Nature 358: 42
5. Salama F, Bakes ELO, Allamandola LJ, Tielens AG (1996) Astrophys J 458: 621
6. Salama F, Galazutdinov GA, Krelowski J, Allamandola LJ, Musaev FAE (1999) Astrophys J 526: 265
7. Harvey RG (1996) Polycycl Aromat Comp 9: 1
8. Palackal NT, Burczynski ME, Harvey R, Penning TM (2001) Biochemistry 40: 10901
9. Velázquez J, Bolobоueva LA, Cool TA (1998) Combust Sci Technol 134: 139
10. Kanda Y, Shimada R (1959) Spectrochim Acta 15: 211
11. Koch EE, Otto A (1969) Opt Commun 1: 47
12. Hohlneicher G, Börsch-Pulm B (1987) Ber Bunsenges Phys Chem 91: 929
13. Klevens HB, Platt JR (1949) J Chem Phys 17: 742
14. Klevens HB (1950) J Chem Phys 18: 1063
15. (1966–1971) Atlas of organic compounds. Butterworths, London
16. Dick B, Hohlneicher G (1983) Chem Phys Lett 97: 324
17. Soos ZG, Hayden GW (1989) Synth Met 28: D543
18. Nakamura Y, Tsuihiji T, Mita T, Minowa T, Tobita S, Shizuka H, Nishimura J (1996) J Am Chem Soc 118: 1006
19. Swiderek P, Michaud M, Hohlneicher G, Sanche L (1991) Chem Phys Lett 178: 289
20. Hochstrasser R, Small GJ (1966) J Chem Phys 66: 2270
21. Syassen K, Philpott MR (1978) J Chem Phys 69: 1251
22. Otokozawa H, Inomata S, Mikami N, Ito M (1977) Bull Chem Soc Jpn 50: 2899
23. Thulstrup EW, Michl J, Eggers JH (1970) J Phys Chem 74: 3868
24. Efremov NA, Kulikov SG, Personov RI, Romanovskii YV (1988) Chem Phys 128: 9
25. Salama F, Joblin C, Allamandola LJ (1994) J Chem Phys 101: 10252
26. Gudipati MS, Daverkausen J, Maus M, Hohlneicher G (1994) Chem Phys 186: 289
27. Husain MM, Kahn MS, Kahn ZH (2000) Spectrochim Acta A56: 2741
28. Hoshi T, Inoue H, Tanizaki Y, Yoshino J, Masamoto T (1972) Z Phys Chem 81: 23
29. Vasak M, Whipple MR, Michl J (1978) J Am Chem Soc 47: 6867
30. Henry BR, Kasha M (1967) J Chem Phys 47: 3319
31. Lavalette D, Tetreau C (1974) Chem Phys Lett 29: 204
32. Hoshi T, Ota K, Shibuya E, Murofushi K (1975) Chem Lett 137
33. Kuball HG, Euing W (1975) Chem Phys Lett 30: 457
34. Kryschi C, Kupka H, Perkampus HH (1987) Chem Phys 116: 53
35. Gritsan NP, Korolev VV, Sushkov DG, Khmelinski IV, Bazhin NM (1990) J Lumin 46: 311
36. Pavlopoulos TG (2002) J Photochem Photobiol A 149: 45
37. Schaaf R, Perkampus HH (1980) Tetrahedron 37: 341
38. Bréchignac P, Pino T, Boudin N (2001) Spectrochim Acta 57: 745
39. Obenland S, Schmidt W (1975) J Am Chem Soc 97: 6633

40. Clar E, Schmidt W (1976) Tetrahedron 32: 2563
41. Schmidt W (1977) J Chem Phys 66: 828
42. Platt JR (1949) J Chem Phys 17: 489
43. Dasgupta A, Chatterjee S, Dasgupta NK (1978) J Indian Chem Soc 55: 935
44. Chakrabarti A, Ramasesha S (1996) Int J Quantum Chem 60: 381
45. Nishimoto K, Forster LS (1965) Theor Chim Acta 3: 407
46. Weltin E, Weber JP, Heilbronner E (1964) Theor Chim Acta 2: 114
47. Bloor JE, Gibson BR, Brearley N (1967) Theor Chim Acta 8: 35
48. Pariser R (1956) J Chem Phys 24: 250
49. Thulstrup EW, Case PL, Michl J (1974) Chem Phys 6: 410
50. Niederalt C, Grimme S, Peyerimhoff SD (1995) Chem Phys Lett 245: 455
51. Andersson K, Malmqvist P-Å, Roos BO, Sadlej AJ, Wolinski K (1990) J Phys Chem 94: 5483
52. Andersson K, Malmqvist P-Å, Roos BO (1992) J Chem Phys 96: 1218
53. Roos BO, Fülscher MP, Malmqvist P-Å, Merchán M, Serrano-Andrés L (1995) In: Langhoff SR (ed) Quantum mechanical electronic structure calculations with chemical accuracy. Kluwer, Dordrecht, The Netherlands, pp 357
54. Roos BO, Andersson K, Fülscher MP, Malmqvist P-Å, Serrano-Andrés L, Pierloot K, Merchán M (1996) In: Prigogine I, Rice SA (eds) New methods in computational quantum mechanics. Advances in chemical physics vol XCIII Wiley, New York pp 219
55. Merchán M, Serrano-Andrés L, Fülscher MP, Roos BO (1995) In: Hirao K (ed) Recent advances in multireference theory, vol IV. World Scientific, Singapore, pp 161
56. Pierloot K, Dumez B, Widmark P-O, Roos BO (1995) Theor Chim Acta 90: 87
57. Rubio M, Merchán M, Ortí E, Roos BO (1994) Chem Phys 179: 395
58. Rubio M, Merchán M, Ortí E, Roos BO (1995) Chem Phys Lett 234: 373
59. Roos BO, Andersson K, Fülscher MP, Serrano-Andrés L, Pierloot K, Merchán M, Molina V (1996) J Mol Struct (THEOCHEM) 388: 257
60. Malmqvist P-Å (1986) Int J Quantum Chem 30: 479
61. Malmqvist P-Å, Roos BO (1989) Chem Phys Lett 155: 189
62. Frisch MJ, Trucks GW, Schlegel HB, Gill PMW, Johnson BG, Robb MA, Cheeseman JR, Keith T, Petersson GA, Montgomery JA, Raghavachari K, Al-Laham MA, Zakrzewski VG, Ortiz JV, Foresman JB, Cioslowski J, Stefanov BB, Nanayakkara A, Challacombe M, Peng CY, Ayala PY, Chen W, Wong MW, Andres JL, Replogle ES, Gomperts R, Martin RL, Fox DJ, Binkley JS, Defrees DJ, Baker J, Stewart JP, Head-Gordon M, Gonzalez C, Pople JA (1995) Gaussian 94. Gaussian, Pittsburgh, PA
63. Andersson K, Blomberg MRA, Fülscher MP, Karlstöm G, Lindh R, Malmqvist P-Å, Neogrády P, Olsen J, Roos BO, Sadlej AJ, Schütz M, Seijo L, Serrano-Andrés L, Siegbahn PEM, Widmark P-O (1997) MOLCAS version 4.0. University of Lund, Lund, Sweden
64. Serrano-Andrés L, Roos BO (1996) J Am Chem Soc 118: 185
65. Beck ME, Rebentisch R, Hohlneicher G, Fülscher MP, Serrano-Andrés L, Roos BO (1997) J Chem Phys 107: 9464
66. Hohlneicher G, Dick B (1979) J Chem Phys 70: 5427
67. Kawashima Y, Hashimoto T, Nakano H, Hirao K (1999) Theor Chem Acc 102: 49
68. Baiardo J, Mukherjee R, Vala M (1981) Appl Spectrosc 35: 510
69. Gallivan JB, Brinen JS (1969) J Chem Phys 50: 1590
70. Del Barrio JI, Rebato JR, Tablas FMG (1986) J Phys Chem 90: 2811
71. Bréchignac P, Pino T (1999) Astron Astrophys 343: L49